Journal of Engineering and Applied Sciences 14 (23): 8676-8685, 2019
ISSN: 1816-949X

A Case Study of the Ground Collapse Mechanism Due to Excavation-Induced Groundwater Level Disturbance

[1]Y. Han, [2]J. Kim, [3]H. Jang, [4]H. Sohn and [1]K. Yoo
[1]Department of Geotechnical Engineering Research, Institute of Korean Geotechnical Society, Seoul, South Korea
[2]Department of Civil, Environmental and Architectural Engineering, University of Padova, Padua, Italy
[3]Research Division of Archaeology, National Research Institute of Cultural Heritage, Daejeon, South Korea
[4]Department of Research and Development, JIYUN EnC Co., Ltd, Seoul, South Korea
shikrush@naver.com

Abstract: Cities are now experiencing accidents with unpredicted ground collapses adjacent to the existing properties. Such ground collapses, caused by natural or artificial factors, may harm the assets in dense urban areas. This study discusses the ground collapse induced by groundwater level disturbance in an excavation site. The subsurface condition was characterized by geophysical methods; ground loosening region around the excavation site was detected and analyzed by Real Time Kinematic (RTK), Ground Penetrating Radar (GPR) and Electrical Resistivity Tomography (ERT). To overcome the unreliability or ambiguity problems in the interpretation results, interpretations of the ERT and GPR data are compared and then, integrated for detection of the water leakage in this case study. The survey results showed a wide range of adjacent ground was loosened due to groundwater drawdown. A numerical analysis in MODFLOW was carried out to simulate the groundwater flow on the site. Finally, it can be concluded that the soil erosion due to water leakage and the positive groundwater discharge was the main contributing factor of the collapses. The initial ground improvement plan of high pressure grouting, therefore had to be replaced by low pressure grouting to avoid any further soil erosion that would eventually lead to potential collapses on the adjacent site.

Key words: Electrical Resistivity Tomography (ERT), geophysical methods, ground collapse, groundwater flow, Ground Penetrating Radar (GPR), soil ersion

INTRODUCTION

As a consequence of rapid urbanization, the need of large-scale ground excavation work for infrastructures and buildings in the cities is greater than ever. Such large-scale excavation can cause unpredicted ground collapses adjacent to the existing properties in dense urban areas. Sinkholes forming on the roads in particular are problematic, since, they can deteriorate the existing structures and even harm the people in the area. It is therefore, necessary to study the causes of sinkholes in the cities to mitigate the potential risk.

A sinkhole refers to a phenomenon whereby the ground surface sinks to create a cylinder or funnel shape on the ground after the underground cavity has collapsed. The cause of sinkholes due to the collapse of the underground cavity can be categorized into two types, sinkholes due to natural process and those induced by human interventions such as constructions on the adjacent site.

Sinkholes generated due to natural process develop as follows: acidification of surface water occurs when surface water absorbs carbon dioxide or participates in the metabolic activities of plants and such acidified surface water flows through bed rocks and weakens the structural integrity of the rocks. In particular when bed rocks are composed of soft minerals such as limestone or carbonate rock, weakening of the structural integrity becomes more severe. Some of the typical types of naturally-caused sinkholes are ground collapse, ground subsidence and ground dissolution (Han and Hwang, 2017).

Corresponding Author: Y. Han, Department of Geotechnical Engineering Research, Institute of Korean Geotechnical Society, Seoul, South Korea, shikrush@naver.com

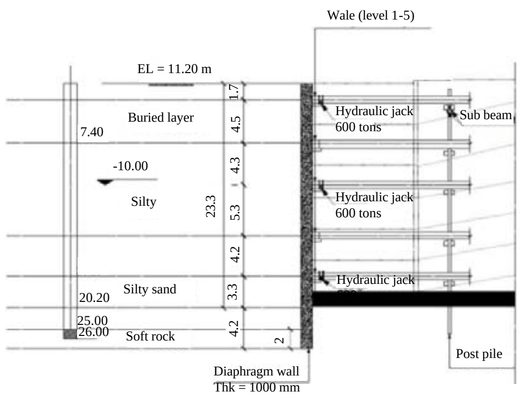

Fig. 1: Sectional view of the excavation plan

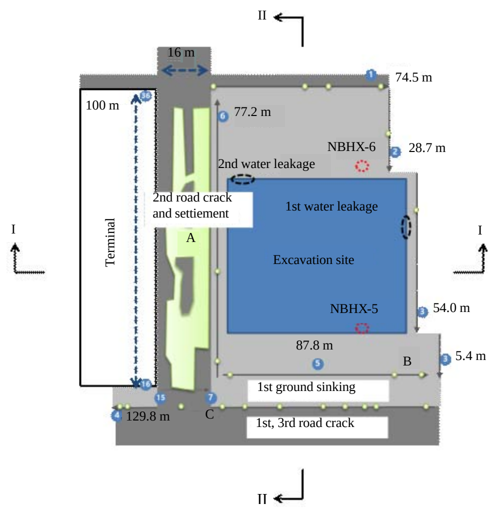

Fig. 2: Outline of the ground sinking in the OO area in South Korea

On the other hand, artificial sinkholes are generated by cavity expansion due to loosened ground and collapse during the underground construction of structures such as tunnels, underground cavity expansion due to defective compaction of backfill materials during construction of structures and erosion due to water leakage in urban water supply and drainage pipes followed by expansion of an underground cavity and underground water disturbance (Han and Hwang, 2017).

Between the two, the human-made sinkholes are more of concerns in an urban setting where an excavation is carried out. A previous research classifies the major factors that contribute to the ground collapse in Korea during excavation as insufficient ground survey, unstable temporary facility structure, instability of the excavation floor surface due to boiling and heaving, instability due to inadequate groundwater treatment (e.g., water stoppage of blocking and drainage), errors in the execution of works, collapse due to excessive excavation, collapse due to slope failure and collapse due to negligent management (K0IST., 2010).

The scope of this study is limited to artificial sinkholes due to excavation with a case in which groundwater discharge induced ground collapse by changing the groundwater flow and thus, increasing the effective stress within the surrounding area during the excavation work of a large-scale building. The loosening of ground was detected using geophysical methods such as GPR, ERT and Real Time Kinematic (RTK).

A case study in Korea: A series of ground collapses and damages adjacent to an excavation site in Korea was reported during groundwork. Figure 1 shows the subsurface ground condition of the excavation site in the OO area. The buried layer just below the ground surface is composed of loose sand and gravel mixed with silt with an average N-value of 6. This layer is approximately 7.5 m thick. Below the buried layer is a layer of silty Sand (SM) up to 22.5 m. It is a very solid layer with an average N-value of 15. Then, very dense gravelly sand with an average N>30 is encountered up to 25.0 m and soft rock is encountered below the gravelly sand. In addition, the groundwater level is located 10.0 m below the ground surface.

A diaphragm wall was used as a support of excavation. Such a retaining wall is constructed by stabilizing the excavation cut using liquid stabilizer, followed by the insertion of mesh reinforcement and the concrete placing. This method has outstanding advantages of high rigidity and groundwater cutoff. Thus, the retaining wall is appropriate for cases in which a large load is applied or ground deformation is expected.

High pressure grouting was used initially within the soils around the perimeter to stabilize the silt layer and to provide a cut off to control groundwater. However, this method is generally not suitable for silty or silty sand layers, since, the excessive pressure of the grouting can cause fractures in the loosened layer.

In the first stage of the ground sinking and road crack, groundwater was discharged from the first water leakage joint of the diaphragm wall that is 20 m below the ground surface (Fig. 2) at around 2:40 p.m., February 6, 2017 and the groundwater level decreased by 1.0 m. In the first ground sinking occurrence region (Fig. 3), a ground sinking of 3 m in length and 30 cm in depth took place and a crack of 30 m in length and 0.05-0.1 m in width was formed (Fig. 3b).

Fig. 3: Ground sinking occurrence site in the OO area in South Korea: a) First ground sinking; b) First road crack; c) Second road crack and settlement and d) Third road crack

In the second stage of the road crack and settlement, groundwater was discharged from the second water leakage joint of the diaphragm wall that is about 20 m below the ground surface (Fig. 3a) at around 6:30 pm., February 14, 2017, during the reinforcement work in relation to the first accident and the groundwater level decreased by about 6.0 m. In the second ground settlement occurrence region (Fig. 3b), a road crack and settlement that was 100 m in length were formed (Fig. 3c). In the case of the third road crack event, a crack that was 20 m in length and 0.03-0.05 m wide was formed in the same region where the initial ground sinking event occurred at around 3:20 pm, February 22, 2017 (Fig. 3d).

MATERIALS AND METHODS

Geophysical methods: Geotechnical and engineering applications of surface geophysical techniques have gained wide interest in the last few decades. This is evidenced by the intensive research and exploration works using Electrical Resistivity Tomography (ERT), Ground Penetrating Radar (GPR) and other electromagnetic techniques. These methods are quick, cheap and non-invasive. It can be used to provide information about the geotechnical conditions and detect zones of cavities or voids (KSEEG., 2008; Reynolds, 2011).

Ground Penetrating Radar (GPR): GPR is a geophysical method to obtain the high resolution information to a depth of typically 0-20 m are possible in some geotechnical environments. The technique is nondestructive and noninvasive, utilizing non-sinusoidal electromagnetic waves with frequencies ranging from 10 MHz to 4 GHz (Reynolds, 2011).

In the plane-wave solution of Maxwell's equations, the electric field E of and electromagnetic wave that is travelling in z-direction is expressed as Takahashi *et al*. (2012) Eq. 1:

$$E(z,t) = E_0 e^{j(\omega t - kz)} \quad (1)$$

where, E_0 is the peak signal amplitude, • is the angular frequency and $k = \omega\sqrt{\varepsilon\mu}$ the wave number. The propagation velocity v of the electromagnetic wave in soil is characterized by the dielectric permittivity and magnetic permeability of the medium:

$$v = \frac{1}{\sqrt{\varepsilon\mu}} \quad (2)$$

Where:

• = The dielectric constant
μ = The magnetic permeability

Radio reflections from targets in the ground are detected by the receiver unit, amplified and displayed by the control unit. Reflections occur where there is a change in the dielectric properties of two adjacent layers across a soil boundary or a material interface (Yelf, 2007).

Velocity information is also commonly derived by the analysis of the shape of hyperbolic reflections from subsurface targets such as pipes or cables. Targets are recognized and classified with reference to the objectives of the survey. Reflections on the GPR profiles are interpreted as geological boundaries, pipes, buried objects, voids and cavities.

Electrical Resistivity Tomography (ERT): ERT methods are characterized by high effectiveness of surveying because electrical resistivity is a parameter which can highly illustrate diversity of a ground condition, considering lithological and hydrological aspects (Reynolds, 2011).

An electrical current is injected into the ground through short steel electrodes distributed along a straight line and the resistance values between the injection points are measured. By careful and correct processing, a two-or three-dimensional resistivity profile of the ground is derived.

In a homogeneous and isotropic half-space, the injected current density J has then to be calculated for all the radial directions with Eq. 3:

$$J = \frac{1}{2\pi r^2} \quad (3)$$

Where:

I = The electrical current and

$2• r^2$ = The surface of a hemispherical sphere of radius r

The potential V can be expressed in Eq. 4:

$$V = \frac{\rho 1}{2\pi r} \quad (4)$$

where, • is the electrical resistivity. Measurement of electrical resistivity usually requires four electrodes: two electrodes called A and B that are used to inject the current ("current electrodes"). The potential difference • V measured between the electrodes M and N is given by Eq. 5:

$$\Delta V = \frac{\rho 1}{2\pi}\left[\frac{1}{AM}-\frac{1}{BM}-\frac{1}{AN}+\frac{1}{BN}\right] \quad (5)$$

where, AM, BM, AN and BN represent the geometrical distance between the electrodes A and M, B and M, A and N and B and N, respectively. The electrical resistivity is then Eq. 6:

$$\rho = K\frac{\Delta V}{I} \quad (6)$$

where, K is a geometrical coefficient that depends on the arrangement of the four electrodes A, B, M and N (Samouelian *et al*., 2005). The resistivity (inverse of conductivity) is often highly varying between ground materials of different types. While clay is one of the most conducting substances to be found, quick clay, other sediments, soft rock and hard rock have all higher resistivity and can be distinguished. This method can reveal the structure of the electrical resistivity to a depth of several tens of meters.

Real Time Kinematic (RTK): RTK can be used to enhance the precision of position data of ground collapse derived from satellite-based positioning systems. It relies on a single reference station or interpolated virtual station to provide real-time corrections, providing up to centimeter-level accuracy.

One of common problems in interpretation of geophysical data is the unreliability or ambiguity in the interpretation results. As a fact when utilizing the geophysical techniques in order to study the subsurface conditions of any excavation site it is strongly recommended or necessary to use two or more geophysical techniques to provide more detailed information about the subsurface structures and lithology.

Groundwater flow analysis: The groundwater level drawdown resulting from the groundwater discharge from an excavation site was analyzed through a numerical analysis using Visual MODFLOW (A Modular 3-D Finite Difference Groundwater Flow Model) Ver. 4.2, a widely used 3-D numerical model. MODFLOW may simulate the groundwater flow in a saturated zone, based on the following assumptions.

The simulated domain is a saturated zone and the aquifer is not changed to a porous medium. The flow is incompressible and the groundwater system is under the isothermal condition. The following governing equation derived from the continuum equation and Darcy's law is used for the simulation of the groundwater flow after finite difference discretization Eq. 7:

$$\frac{s}{b}\frac{\partial h}{\partial t} = \frac{\partial}{\partial X_i}\left(K_{ij}\frac{\partial h}{\partial X_j}\right) \pm Q \quad (7)$$

Where:

K_{ij} = The hydraulic conductivity tensor

h = The dynamic head

Q = The source/sink

S = The storage coefficient

b = The aquifer thickness

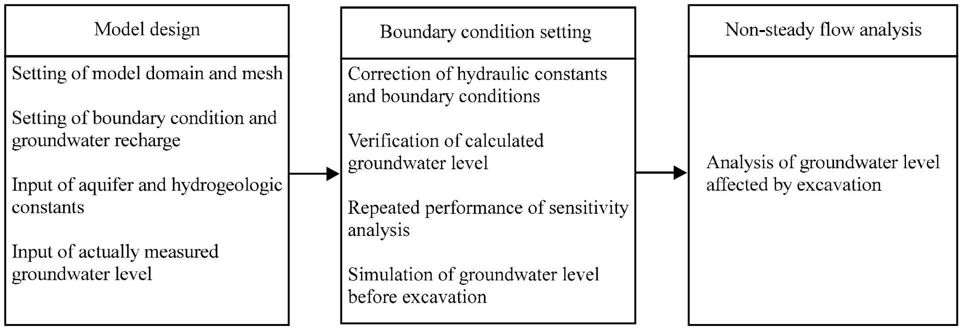

Fig. 4: Stages of groundwater flow analysis

An analysis of the groundwater flow using the modeling software can be divided into the three stages shown in Fig. 4. Stage 1 is the design of an optimized model that is simplified in order to understand the dominant processes in the groundwater flow system. In stage 2, the findings obtained through observation are compared with the results of a simulation to verify the calculated groundwater level by correcting the hydraulic constants and the boundary conditions through the trial-and-error method or automatic regression. Stage 3 is the final stage of the model application in which the variation in the groundwater level and the effect of the variation are predicted on the basis of the simulation results obtained by correction.

The analytical domain is near to the boundaries representing Dochon Stream, Pungdong Stream and Janghang Stream with the excavation location at the center. The mesh for the modeling was 6.4 km long in the East-West direction and 5.6 km long in the North-South direction including the excavation area. The mesh was generated as an irregular mesh including 5 m grids around the excavation area and 10, 20 and 40 m grids in the areas that are not significantly affected by the groundwater discharge. The riverbed boundaries and the boundary conditions set for the model were no-flow boundary condition, considering the groundwater divide along the ridge line from the zenith (Mt. Jeongbal). In addition, Ilsan Lake Park was set as a general head boundary and the Han River was input as a river boundary. Small streams such as Dochon Stream, Pungdong Stream and Janghang Stream were set as drain boundaries (Fig. 5).

The groundwater recharge was estimated based on the data in the literature. Considering that the ground surface of most of the excavation area is covered with asphalt and concrete which means that hardly any rainfall infiltrates and the runoff is high, the groundwater

Fig. 5: Boundary condition setting

Table 1: Hydraulic constants

Items	Values
Groundwater recharge (mm/year)	63.5
Hydraulic constant	
Permeability coefficient (cm/sec)	3.14×10-3
Sedimentary layer	8.00×10-4
Colluvium	3.00×10-4
Rock layer	0.01
Storage coefficient	
Boundary condition	
GHD	Ilsan Lake Park
River	Han River
Drain	Dochon, Pungdong and Janghang Streams

recharge of 4.83% was applied, referring to the Natural Resources Conservation Service-Curve Number (NRCS-CN) runoff analysis method. Therefore, the runoff was determined as 63.5 mm/year which is 4.83% of the 10 years average precipitation at the observation post near to the excavation area (1,314 mm/year) (Table 1).

The ground bed around the excavation area included the top reclamation layer and a thick sedimentary layer, under which there was a partial weathering zone of 1.0-2.2 m. A soft rock layer was found under the weathering zone. Therefore, the individual hydraulic constants used for the analysis were calculated through the model correction, referring to the results of on-site tests and the data from the literature.

RESULTS AND DISCUSSION

Geophysical surveys results: An RTK (Real Time Kinematic) survey was conducted for the area A shown in Fig. 6. The elevations of the ground surface were measured for the dots as shown in Fig. 6. The result showed that the ground surface had sunk and formed a bowl shaped surface.

The surrounding areas of the excavation site in Fig. 2 were examined using a GPR exploration equipment (Mala 450 MHz) and ERT on February 21, 2017. The result of these geophysical methods showed that the surrounding ground of the excavation had been loosened. In particular, the ground loosening region was found to be widely distributed underneath the road of the second ground settlement occurrence region (Fig. 7 and 8). Figure 7a-c show the result from the area A, B and C marked in Fig. 2, respectively.

Groundwater flow analysis result: In the simulation of a groundwater flow, it is generally, impossible to input all the complex information involved in an actual site to a mode. Therefore, the actual site situation should be simplified to a certain degree for conceptualization which requires correction of the model. In the present study, the

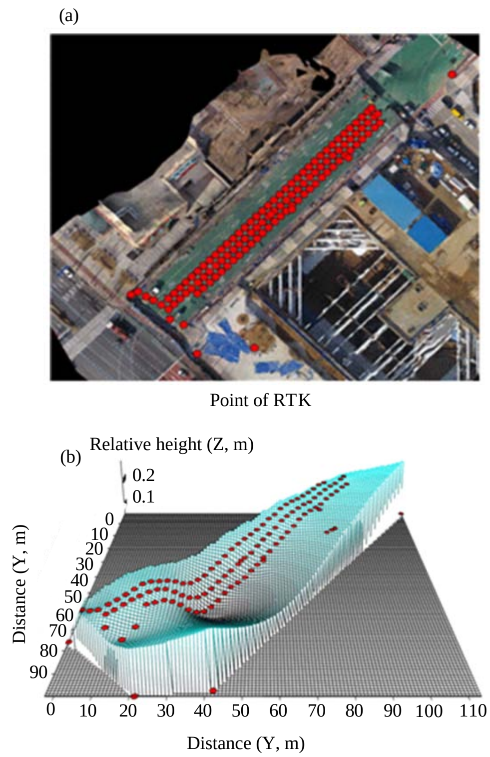

Fig. 6: a, b) RTK survey result

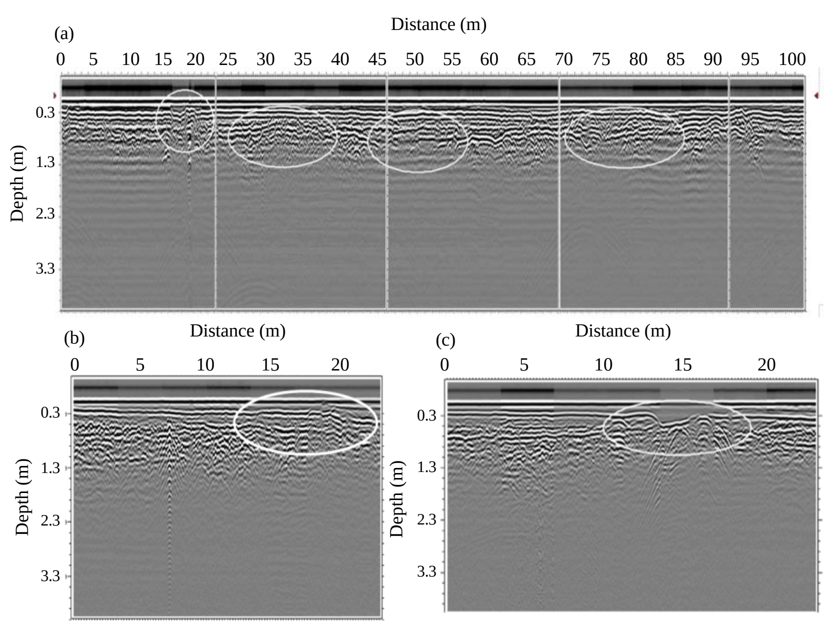

Fig. 7: a-c) GPR exploration result (Han and Yoo, 2017)

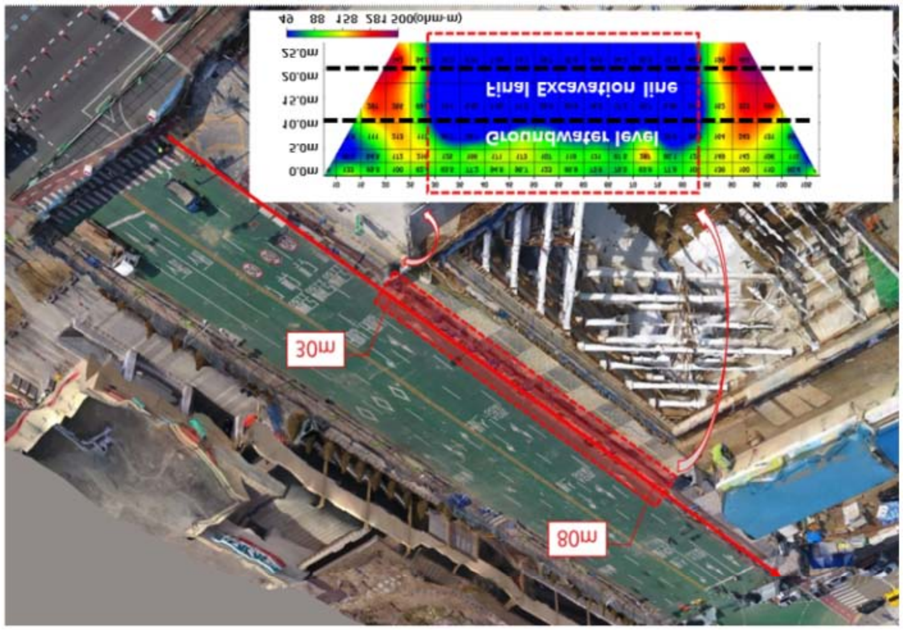

Fig. 8: ERT survey result

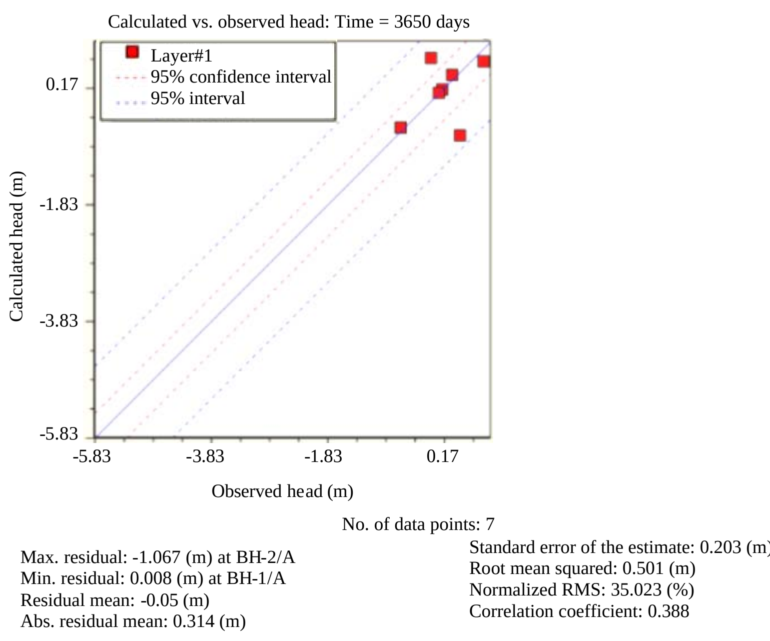

Fig. 9: Result of model correction for non-steady state

model was corrected using the groundwater level data measured at five boreholes excavated for the observation of the geological information and the groundwater level in the excavation area. The observation showed that the groundwater level in the excavation area was approximately 10 m below the ground's surface (Fig. 8). The model was corrected using the on-site observation head and the calculated head. As shown in Fig. 9, the average residual was -0.05 m and the average error was 0.203 m indicating that the present analytical model well-reflected the groundwater level of the excavation area to appropriately predict the groundwater level variation during excavation. To simulate the non-steady state of the groundwater level variation in the surrounding areas due

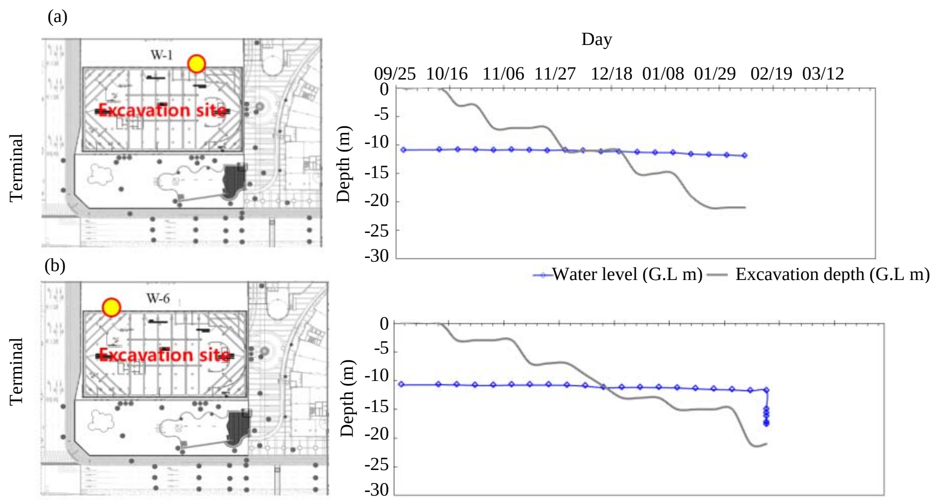

Fig. 10: Groundwater monitoring result

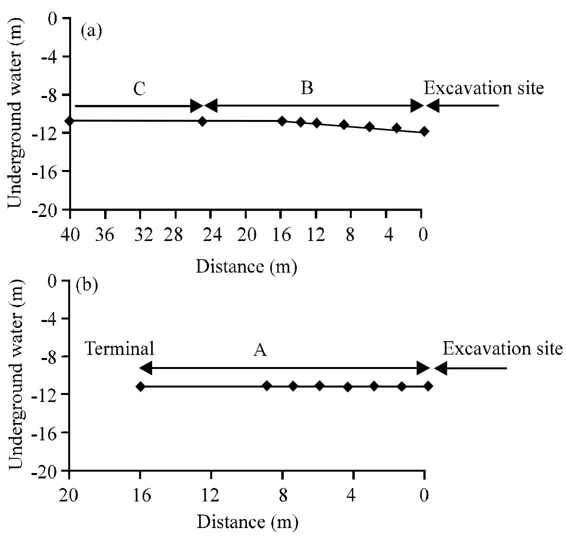

Fig. 11: a, b) Area affected by first water leakage; I-I Section

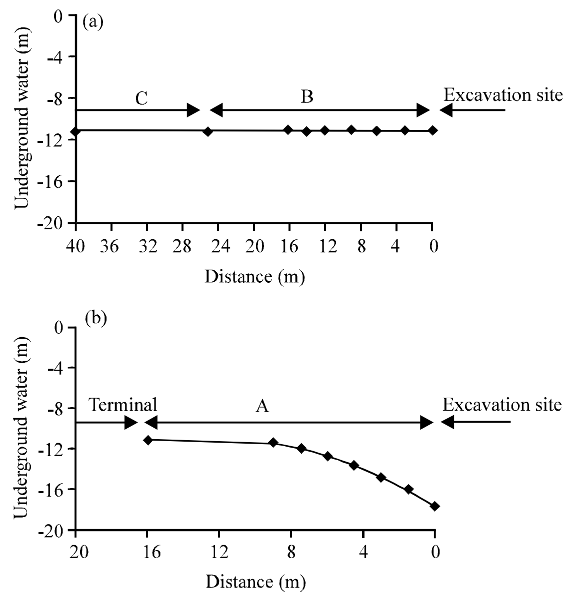

Fig. 12: a, b) Areas affected by second water leakage

to ground improvement work, a non-steady state analysis was performed from the leakage points that directly affect the groundwater flow. Excavation cutoff walls and drainages were installed at the excavation site and underground walls were installed at the OO Terminal and Bella city to establish perfect cutoff conditions.

The observation head (Fig. 10) was set up as the initial groundwater level for the non-steady state to analyze the variation of the groundwater level depending on the ground improvement work leakage on the individual days of water leakage (Fig. 11 and 12).

The analysis showed that the groundwater level was lowered in areas B and C of (Fig. 2) due to the first leakage (February 6, 2017) (Fig. 11), resulting in cracks and subsidence on the road near to the excavation site as shown in Fig. 3a and b. The second leakage (February 14, 2017) significantly lowered the groundwater level in area A of Fig. 2 (Fig. 12), resulting in subsidence on the roads around the excavation site, as shown in Fig. 3c.

Grouting: Although, the initial construction plan only included high pressure grouting around the excavation area, it was replaced by low pressure grouting in the middle of construction to avoid additional soil erosions that can cause further ground collapse. Figure 13 shows the final grouting plan with low and high pressure grouting around the walls. The road crack and ground collapse were observed after the first stage of high

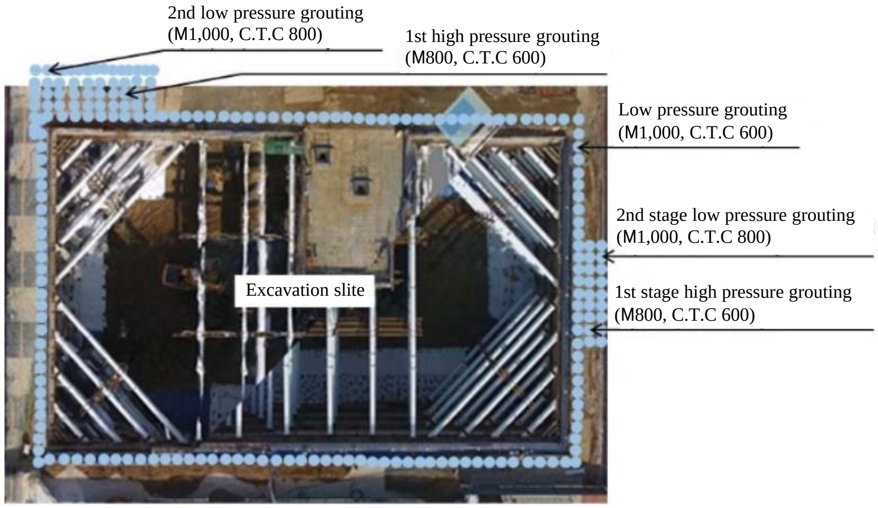

Fig. 13: Ground improvement

pressure grouting at the eastern and Northwestern part of the walls. Low pressure grouting was then conducted at the second stage for the outer part of high pressure grouted area. In addition, low pressure grouting was conducted throughout the entire perimeter of the excavation site.

CONCLUSION

The sinkholes formed in the OO area in Korea were mainly induced by groundwater level disturbance. The following conclusions can be drawn in relation to the cause of the accidents.

In the OO area where the ground collapsed, a water vein is located at a depth of 10-20 m. It can be concluded that the ground collapses occurred in the surrounding area due to soil erosion at some part of the walls with groundwater leakage. The water leakage was induced by poor installation of a diaphragm wall during the excavation work.

The geophysical surveys (GPR, ERT and RTK) found that the ground around the excavation was loosened due to the groundwater discharge at the site and the ground loosening region was found to be widely distributed over the surrounding ground with a groundwater level of >6.0 m.

There is a concern about long-term damage, since, the ground loosening region is widely distributed around the ground excavation site.

The result from the groundwater flow analysis showed that the observed ground collapses coincided with the ground improvement works, indicating that excessive pressure from grouting had lowered the groundwater level significantly. Considering the results from the GPR, ERT and RTK measurements, high pressure grouting was replaced by low pressure grouting to stabilize the silt and silty sand layer and to ensure a groundwater cutoff.

In the light of the geophysical survey results and the groundwater flow analysis result, the initial plan of high pressure grouting was replaced by low pressure grouting to avoid any further damages.

Additionally, the findings of this research work indicate that integration of both ERT and GPR data results enhances the accuracy and reliability of detection of geotechnical targets such as the water leakage, cavities.

ACKNOWLEDGEMENT

This research was supported by the Korea Agency for Infrastructure Technology Advancement under the Ministry of Land, Infrastructure and Transport of the Korean government (Project Number: 19SCIP-B108153-05).

REFERENCES

Han, Y. and H.W. Hwang, 2017. Discussion on the sinkhole forming mechanism. Intl. J. Adv. Sci. Eng. Technol., 5: 42-44.

Han, Y. and K.C. Yoo, 2017. Analysis of the ground sinking around an excavation site using GPR exploration. Intl. J. Res. Chem. Metall. Civ. Eng., 4: 206-210.

K0IST., 2010. A research for establishing safety management standards on neighboring facilities in accordance with ground excavation. Korean Infrastructure Safety & Technology Corporation, Jinju-si, South Korea.

KSEEG., 2008. Guidance on geophysical survey. Korean Society of Earth and Exploration Geophysicists Daejeon, Daejeon, South Korea.

Reynolds, J.M., 2011. An Introduction to Applied and Environmental Geophysics. 2nd Edn., Wiley Publishing Company, Hoboken, New Jersey, USA., ISBN:978-0-471-48535-3, Pages: 710.

Samouelian, A., I. Cousin, A. Tabbagh, A. Bruand and G. Richard, 2005. Electrical resistivity survey in soil science: A review. Soil Tillage Res., 83: 173-193.

Takahashi, K., J. Igel, H. Preetz and S. Kuroda, 2012. Basics and Application of Ground-Penetrating Radar as a Tool for Monitoring Irrigation Process. In: Problems, Perspectives and Challenges of Agricultural Water Management, Kumar, M. (Ed.). IntechOpen, London, England, UK., pp: 155-180.

Yelf, R.J., 2007. Application of ground penetrating radar to civil and geotechnical engineering. Electromagn. Phenom., 7: 102-117.